

# Investigation on the Microwave Performance of a High-Speed Opto-Electronic Hybrid Integrated Platform

Wei Han, Marc Rensing, Xin Wang, Peter O'Brien, Frank H. Peters

**Abstract**—An opto-electronic hybrid integrated platform was developed to enable the fabrication of broadband, low-cost, and compact transceivers for telecommunications. On this platform, an opto-electronic device such as a high-speed laser or a photodetector chip is integrated with a RF driver or an amplifier IC. A Kovar heatsink with multistep structure is designed for ease of optical coupling using a laser welding process. In order to control the high frequency resonances and improve the signal integrity, AlN based subcircuits are designed to feed the RF and DC signals separately. The interconnection networks between the IC and the opto-electronic device and also between the chips and high-speed transmission lines are carefully investigated to optimize the microwave performances. The influence of the packaging for this opto-electronic integration platform on the microwave performance is also analyzed in detail. The simulation results obtained and successful fabrication of a transmitter module demonstrate that the proposed platform can meet the requirements for high-speed WDM or TDM systems.

**Index Terms**—Opto-electronic hybrid integration, transceiver module, driver IC, transmission line, RF resonance

## I. INTRODUCTION

As telecommunications demand higher speeds and larger capacities, transmission networks such as time division multiplexing (TDM) and wavelength division multiplexing (WDM) have been studied extensively. Such networks require broadband, compact and low-cost opto-electronic modules such as high-speed modulators and photodetectors. Recent progress in long haul communications and short distance access network systems has already increased the transmission rates to several ten gigabits per second per channel [1, 2]. To meet these requirements, it is important to develop hybrid integrated opto-electronic modules in which semiconductor devices (e.g. amplifiers and driver ICs), opto-electronic devices (e.g. lasers, modulators and PDs) and passive components (e.g. lens, fibers and waveguides) are assembled with RF or DC substrates. Such hybrid integrated platforms are often packaged and encapsulated in metal-ceramic or epoxy resin packages to fulfil different functions such as O/E and E/O

conversions, all-optical 3R regenerations, optical routers and all-optical wavelength assignments [3-5]. The high-level integration will result in a relatively strong signal crosstalk or RF attenuation when the bit rates exceed 10 Gb/s. Especially at frequencies above 40 GHz, high order modes can be easily excited in microwave waveguides and thus generate RF resonance and rapid signal drop-off within the expecting bandwidth.

In this paper, we present an opto-electronic hybrid integrated platform to enable the fabrication of broadband, low-cost, and compact transceivers for telecommunications applications. The proposed system-in package scheme is designed to support differential or dual way RF inputs with the transmission capability of 40 GHz. By building the equivalent circuit model and distributed electromagnetic model of this platform, the residual parameters caused by the bonding wire, IC electrodes, and microwave transmission lines are investigated carefully to restrain the signal attenuations and improve the signal integrities. Likewise the signal crosstalk and high frequency resonances are under deep consideration in RF and DC sub-circuit designs. By assembling this hybrid integrated platform into a butterfly package (BTF), a transceiver module can be constructed for various applications in WDM and TDM systems.

## II. EM ANALYSIS OF OPTO-ELECTRONIC HYBRID INTEGRATED PLATFORM

### A. Schematic Diagram and Circuit Model of the Platform

The proposed opto-electronic hybrid integrated platform is shown in Fig.1 including: an opto-electronic device such as a high-speed laser or a photodetector chip, a RF driver or an amplifier IC, a Kovar heatsink with multistep structure (as shown in the insert of Fig. 1) for easy of optical coupling and laser welding, optical fibre to deliver the optical signals in and out of the module, three sub-circuits to feed the DC and RF signals, and passive elements such as SMT capacitors and resistors. The active chips are fixed on the Kovar heatsink using solder or silver epoxy, and the electronic connections are realized by wire and ribbon bonding. The block diagram of the platform is shown in Fig.2a, in which an E/O modulator and modulator driver IC are used in an optical transmitter. The modulator driver IC has an AC coupling differential input stage. The gain

Wei Han, Marc Rensing, Xin Wang, Peter O'Brien, and Frank H. Peters are with Integrated Photonics Group, Tyndall National Institute, Cork, Ireland (phone: 353-21-420-5637; e-mail: wei.han@tyndall.ie).

Frank H. Peters is with Department of Physics, University College Cork, Co. Cork, Ireland.

This work is supported by SFI grant number 07/SRC/I1173.

control, crossing point adjustment, and output offset control are available. Single-ended output is provided to drive an external E/O modulator. DC decoupling networks are also included in this model, and the undivided stable ground is provided by the Kovar heatsink.

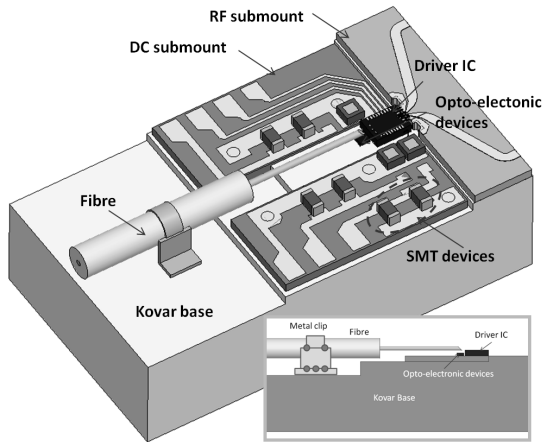


Fig.1 The proposed opto-electronic hybrid integrated platform, insertion show the multistep structure of the Kovar base.

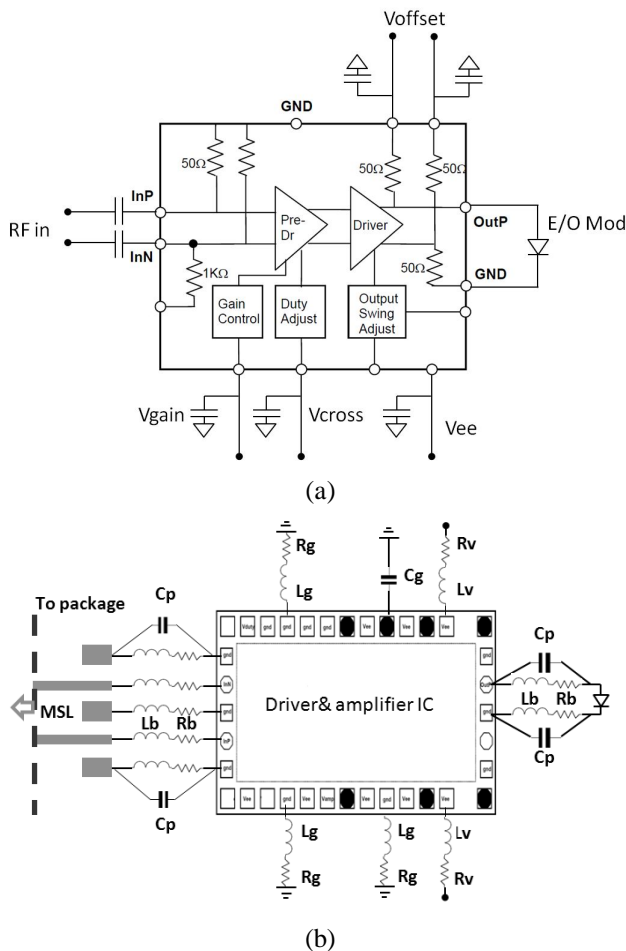


Fig.2 Schematic diagram of the platform circuit (a), circuit model including the parasitical effect of the bonding wires and the IC electrodes (b).

Heat generated in the driver IC is a significant problem in high-speed opto-electronic integrated platforms because the power consumption of the IC will increase drastically

with the operating bit rates. In this paper, the driver IC is assembled with face-up electrical connection for better thermal control. However, the face-up connections of the IC requires wire bonding or ribbon bonding which will bring unwanted parasitic parameters at high frequencies. In Fig.2b, the parasitical effects of the bonding wires and the IC electrodes are added and compared with the circuit scheme in Fig.2a. In the diagram,  $L_b$  and  $R_b$  are the inductance and resistance caused by the ribbon bonding in the RF path;  $R_g$  and  $L_g$  are due to the bonding wire in ground path;  $R_v$  and  $L_v$  are from the power supply path;  $C_p$  and  $C_g$  are the parasitic capacitance between the IC electrodes.

*B. Distributed EM Model of the Platform*

The electrical connection between the chips and circuit are described in Fig.3. In the photograph, a high-speed vertical-cavity surface-emitting laser (VCSEL) is used as an E/O modulator, and the insertion of Fig.1a shows the mesa structure and lasing area of the laser. A GSG type wire connection is employed between the LD and driver IC. Fig.3b shows the pad configuration of the driver IC, and an AIN based RF interface circuit with tapered and grounded coplanar waveguide (TBGCPW) is designed to meet the connection requirement of the IC.

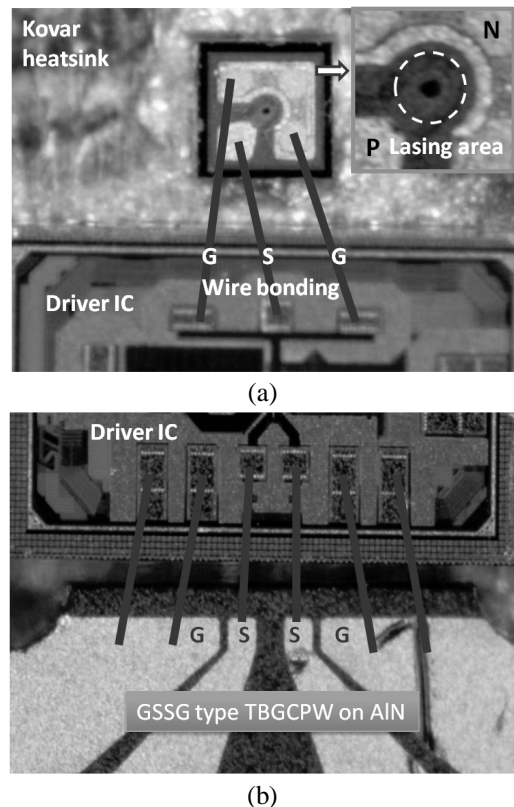
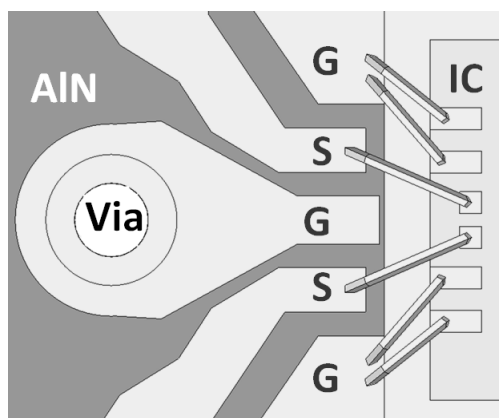


Fig.3 Photograph of the electrical connection between the LD chip and driver IC (a), and between driver IC and RF subcircuits (b).

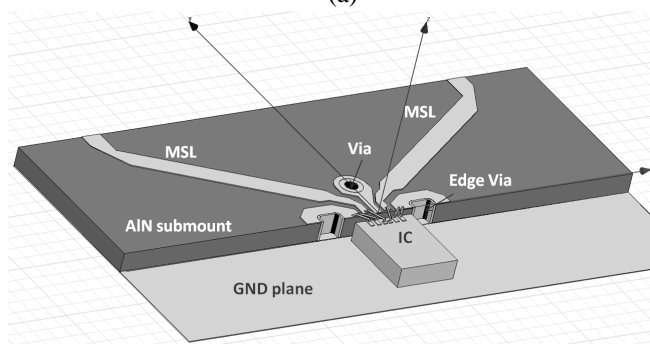
In order to optimize the RF subcircuit and the interconnection between the IC and the circuit, a distributed electromagnetic (EM) model is built using microwave

simulator Ansoft HFSS. As shown in Fig.4, the given RF circuit is based on AlN ceramic with a dielectric constant of 8.7 and loss tangent of 0.002. The RF transmission path is consisted of a microstrip line (MSL) for the connection with the RF connectors, and a coplanar waveguide (CPW) structure for the GSSG pad configuration of the IC.

On the AlN circuit, a through via and two edge vias are employed to form the ground planes. In Fig.4a, a centre ground plane is added between the signal paths to make two GSG pad structures which correspond to the positive and negative data signal inputs of the driver IC. The ratio of the width and the gap of the CPW are set to 0.1 mm/0.05 mm, and the spacing between the IC and circuit is 0.1 mm. The length of the bonding wire is 0.250 mm for the signal paths and 0.2 mm for the ground paths.



(a)



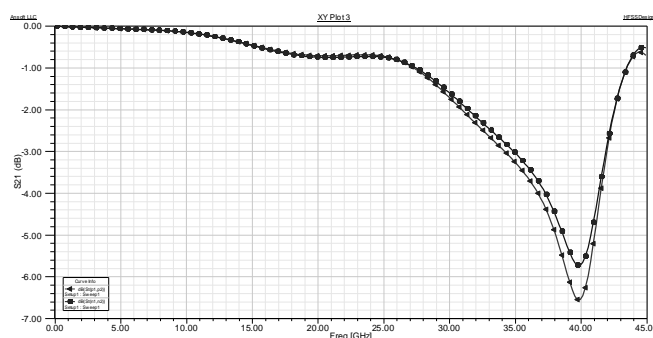
(b)

Fig.4 Pads configuration of the AlN circuit and IC (a); model of the electrical connection between IC and RF circuit (b).

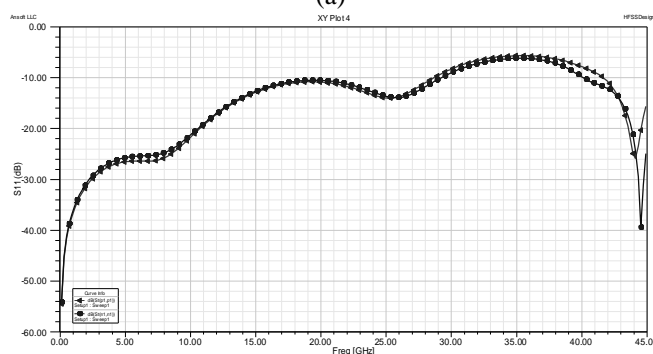
### C. EM Simulation and Analysis on the Platform

Fig.5 gives the simulated frequency response of the interconnection and the assembly of the AlN circuit and driver IC. Strong resonance is observed at 40GHz which brings a signal attenuation of approximately 6dB at 40 GHz and thus limits the -3 dB bandwidth to 34 GHz. In addition, the RF reflection is above -10dB at 28 GHz which will bring more RF return loss due to the impedance mismatch. Furthermore, to investigate the input impedance of the transmission line, time domain impedance analyses are performed. As shown in Fig.4, the RF feed path consists of a MSL and a CPW structure. Two wave ports are assigned

at both ends of the transmission line. In Fig.6, the simulated input impedance shows that on the MSL side, the impedance can be controlled to around 53 Ohm. However, on CPW side, the impedance will increase to 59 Ohm which means a strong impedance mismatch is generated in the GSSG region.



(a)



(b)

Fig.5 Frequency responses of the interconnection and the assembly of the AlN circuit and driver IC, S<sub>21</sub> (a) and S<sub>11</sub> (b); red line: positive input trace; blue line: negative input trace.

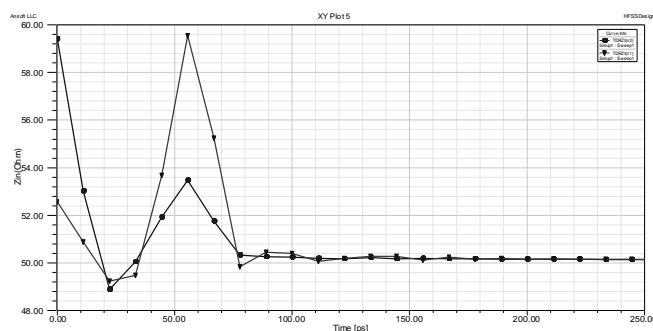


Fig. 6 simulation results on TDR Z<sub>in</sub>; red line: input to the MSL; blue line: input to CPW.

In order to suppress the resonance and increase the bandwidth of the platform, an optimized GSSG type transmission line is designed. In Fig.7, the centre ground plane is removed and the ratio of the width/gap is changed to 0.6 mm/ 0.2 mm for ground and signal paths and 0.6 mm/0.6 mm between signal paths. Moreover, the length of the bonding wire is decrease to 0.2 mm for the signal paths and to 0.15 mm for the ground paths.

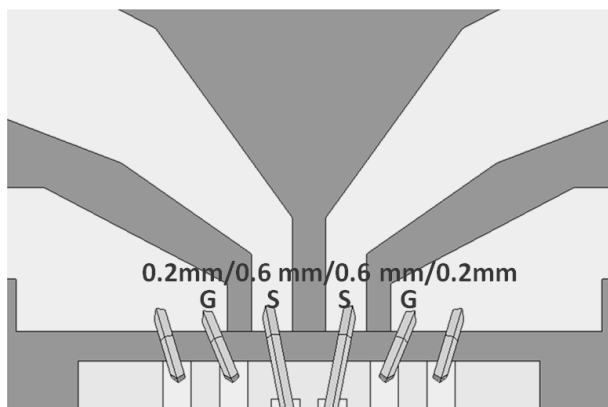


Fig.7 GSSG electrical connection to improve high-frequency performances.

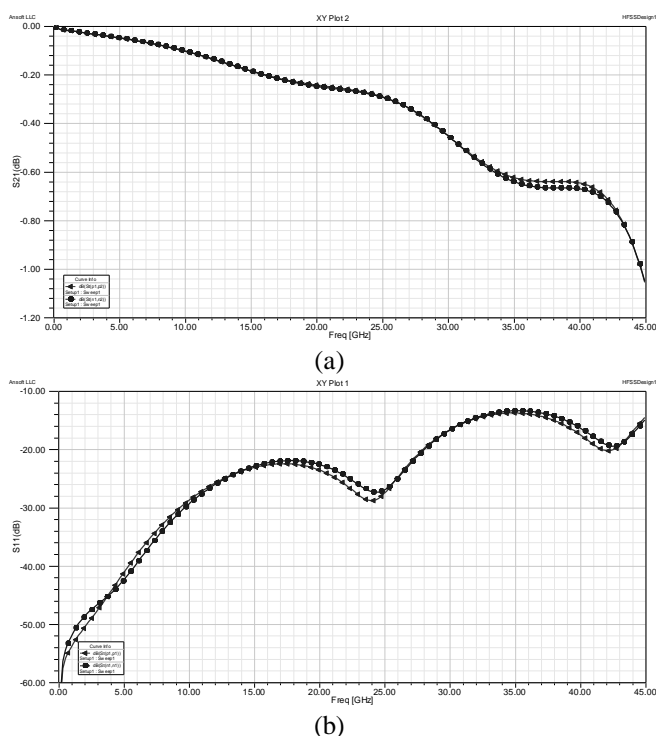


Fig.8 Frequency responses of the interconnection and the assembly of the AIN circuit and driver IC, S21 (a) and S11 (b); red line: positive input trace; blue line: negative input trace.

In Fig.8, the simulated frequency responses show a bandwidth increase as well as RF reflection suppression. The signal attenuation decreases to 0.68 dB at 40 GHz along with a S11 of -14 dB throughout the useful bandwidth. The simulated input impedance in Fig.9 shows an obvious impedance improvement in the GSSG region where it decreases to 55 Ohm. The comparison of the E-field distributions between the GSGSG structure and the GSSG structure is shown in Fig. 10. With respect to GSGSG structure, it can be seen from the plot that a strong resonance is generated between the centre ground plane and the signal path. The symmetric and narrow GSG structure and the impedance mismatch due to the conversion from

MSL to CPW induces strong RF coupling and excites a standing wave in this region. In Fig.10b, the optimized GSSG structure shows relatively low E-field intensity and the coupling between signal lines is designed to be minimized in this region.

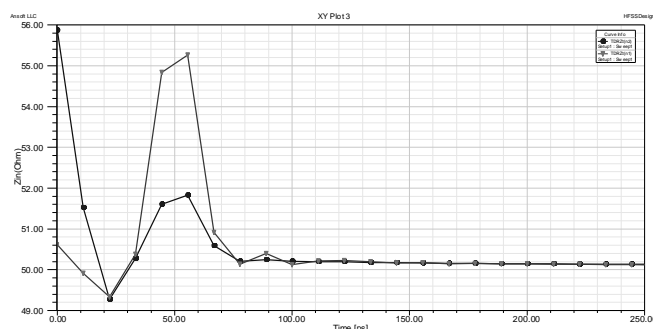


Fig.9 simulation results on TDR Zin; red line: input to the MSL; blue line: input to CPW.

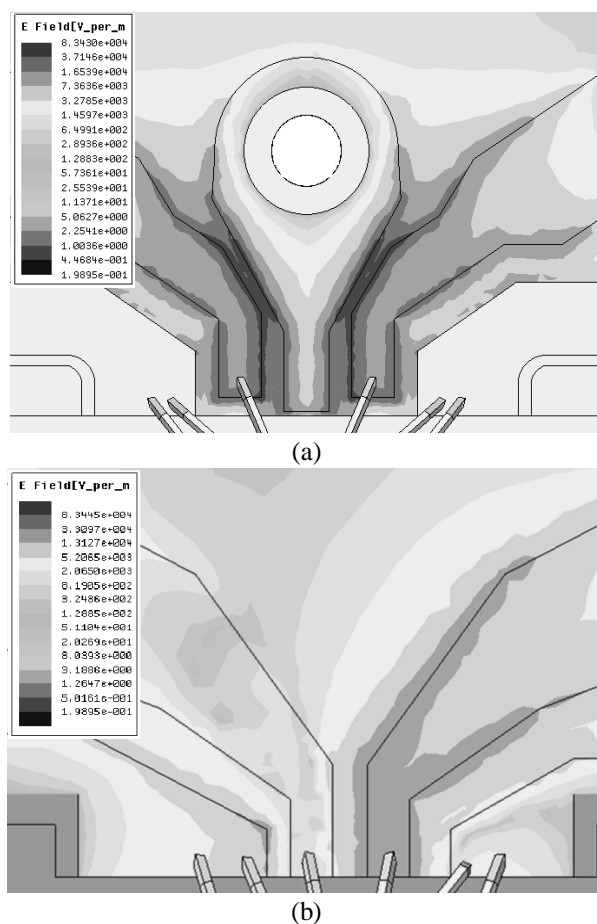


Fig. 10 E-field distributions at 40GHz in GSGSG (a) and GSSG (b).

### III. CONCLUSION

In this paper, we presented an opto-electronic hybrid integrated platform to enable the fabrication of broadband, low-cost, and compact transceivers for telecommunications. The residual parameters caused by the bonding wire, IC electrodes, and microwave transmission lines in this platform were investigated carefully to minimize the signal

attenuation and improve the signal integrities. In order to meet the desired bandwidth of 40 GHz, an optimized RF design was developed to minimize potential frequency decay and resonances. The EM simulation results obtained indicated that the RF signal transmission interface including the RF circuit and the bonding wires has an insertion loss of only 0.68 dB at 40 GHz along with a low RF reflection below -14dB. By assembling this hybrid integrated platform into a butterfly package (BTF) as shown in Fig.11, a transceiver module can be constructed for various applications in WDM and TDM systems.

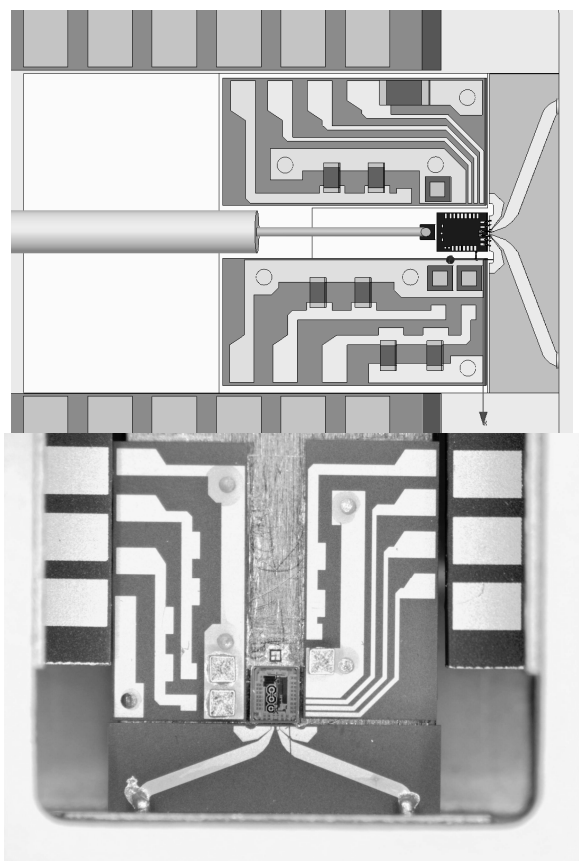


Fig. 11 Schematic diagram and photography of the proposed opto-electronic integrated platform packaged into a BTF to construct a high-speed transmitter module.

#### REFERENCES

- [1] K. Sakai, H. Aruga, S.I. Takagi, M. Kawano, M. Negishi, Y. Kondoh, and S.-I. Kaneko, "1.3  $\mu\text{m}$  uncooled DFB laser-diode module with a coupled differential feed for 10-Gb/s Ethernet application," *J. Lightw. Technol.*, vol. 22, no. 2, pp. 574-581, Feb. 2004.
- [2] D. Frederique, A. Catherine, B. Fabrice, et al. "New Nonlinear Electrical Modeling of High-Speed Electroabsorption Modulators for 40 Gb/s Optical Networks," *J. Lightw. Technol.*, vol. 29, no. 6, pp. 880-887, 2011.
- [3] W. Han, N.H. Zhu, X. Liang, M. Ren, K. Sun, B.H. Zhang, L. Li, and H.G. Zhang, "Injection locked Fabry-Perot laser diodes for WDM passive optical network spare function," *Optics Communications.*, vol. 282, no.17, pp.3553-3557, Sep. 2009.
- [4] Cheng Guan Lim, "Electro-Absorption Modulator Integrated Lasers With Enhanced Signal Injection Efficiency," *J. Lightwave Technol.* Vol. 26, pp. 685-691, 2008
- [5] Peschke. M, Saravanan. B, Hanke. C, Knodl. T, and Stegmuller. B, "Investigation of the capacitance of integrated DFB-EAMs with shared active layer for 40 GHz bandwidth," *Lasers and Electro-Optics Society, 2004. LEOS 2004.* Vol. 2, pp. 673-674, 2004